A Study on the Strong Duality of Second-Order Conic Relaxation of AC Optimal Power Flow in Radial Networks

Xiaoyu Cao, *Member, IEEE,* Jianxue Wang, *Senior Member, IEEE,* and Bo Zeng, *Member, IEEE*

***Abstract*—For the popular second-order conic program (SOCP) formulation of AC optimal power flow (OPF) in a radial network, this paper first shows that it does not have the strong duality property in general. Then, through a series of restrictive reformulations, we derive a set of closed-form sufficient conditions on network parameters that ensure its strong duality. Numerical studies on IEEE 33-bus, 69-bus test networks and two real-world distribution systems confirm that non-negligible duality gaps *do exist* in this SOCP formulation, and also demonstrate the validity of the proposed sufficient conditions on closing the duality gap. Our results provide an analytical tool to ensure the strong duality of the SOCP power flow formulation and to support algorithm developments for its complex extensions.**

***Index Terms*—AC optimal power flow, strong duality, second-order conic program, radial network.**

I. Introduction

THE AC optimal power flow (OPF) model is a fundamental tool for analytical studies of power systems. It is originally nonconvex. Relaxing an AC OPF model into a canonical convex program, e.g., second-order cone program (SOCP) or a semi-definite program (SDP) [1]–[6], enables us to make use of well-developed convex optimization results and algorithms to address this very challenging model. Generally, these convex relaxations can be computed to produce high-quality solutions. Under some sufficient conditions, [6]–[9], they are global optimal or can be used to recover global optimal solutions of the original non-convex AC OPF model. The SOCP formulation is particularly attractive as its computation burden is comparable to that of the vastly adopted linear programming (LP) based DC power flow formulation. Consequently, fast commercial mixed integer SOCP solvers have been used to solve practical instances of SOCP formulation and its more sophisticated extensions in planning, operation, and security analysis, e.g., [10]–[14].

A great advantage of the conventional LP formulation is its *strong duality* property, i.e., it (the primal problem) shares the same optimal value as its dual problem, which is also an LP, when both are feasible. This property has a great significance and provides a substantial support to more advanced studies, including developing fast decomposition algorithms for large-scale power grids, e.g., Benders decomposition and column-and-constraint generation (C&CG) methods, deriving electricity market oriented decisions, and performing vulnerability analysis to identify the critical contingencies. Naturally, it is desired to carry out similar studies using the dual problem of SOCP model, which is also an SOCP, to produce more accurate or realistic results for cases where that the primal model captures the underlying problem better than an LP counterpart.

Indeed, we have noted several existing publications that were developed upon the *dual of SOCP formulation*. Ref [10] developed a Benders decomposition method with SOCP subproblems that captured the nonlinear power flow formulations. The dual problems of those SOCP subproblems were solved to generate Benders cuts. In Ref [11], a bilinear Benders decomposition was adopted to address a distribution network expansion planning (DNEP) problem with stochastic and chance constrained program reformulation. Similar algorithm framework was applied in distributed generation planning [12], energy storage planning [13], and the load restoration decisions for active distribution networks [14]. Besides, Ref [15] designed and implemented a conic-duality based decomposition approach to evaluate the total supply capability of a reconfigurable distribution network. Ref [16] utilized the dual of SOCP in a reactive power management problem to compute the subgradient for a stochastic approximation method.

Additionally, the duality of SOCP plays a central role in simplifying bilevel or trilevel programs, e.g., some substructures of the popular two-stage robust optimization (RO). Ref [17] presented a bilevel model to identify the worst contingency considering the AC OPF represented in an SOCP, which was then converted into a single-level formulation by taking the dual of lower-level SOCP. In Ref [18], a bilevel optimization model was proposed for transmission expansion planning (TEP) problem by using the conic duality to incorporate the market clearing decisions in the lower-level problems. Ref [19] implemented the C&CG algorithm to compute a two-stage RO model for the topology reconfiguration of

This work was supported in part by the National Key R & D Program of China (No. 2018YFB0905000), in part by the Science and Technology Project of SGCC (No. SGTJDK00DWJS1800232), in part by the China Postdoctoral Science Foundation (No. 2019M663722), and in part by the Fundamental Research Funds for the Central Universities (No. xpt012020010 and xxj022019033). The work of Bo Zeng was supported in part by the US National Science Foundation (No. CMMI 1635472).

Xiaoyu Cao is with the School of Automation Science and Engineering and the Ministry of Education Key Lab for Intelligent Networks and Network Security, Xi'an Jiaotong University, Xi'an, Shaanxi 710049 China (e-mail: cxykeven2019@xjtu.edu.cn).

Jianxue Wang is with the School of Electrical Engineering and Shaanxi Key Laboratory of Smart Grid, Xi'an Jiaotong University, Xi'an, Shaanxi 710049 China (e-mail: jxwang@mail.xjtu.edu.cn).

Bo Zeng is with the Department of Industrial Engineering and the Department of Electrical and Computer Engineering, University of Pittsburgh, Pittsburgh, PA 15106 USA (e-mail: bzeng@pitt.edu).

active distribution networks, where the conic duality of AC OPF subproblems was employed. Ref [20] proposed a two-stage RO formulation with mixed-integer SOCP recourse to optimize the routing decisions of mobile de-icing devices for a transmission network (subject to disruptions by ice storms). In this study, a nested C&CG algorithm was adopted, which again relied on the strong duality of SOCP formulation to guarantee the convergence of inner iterations. The dual of SOCP was also involved in Refs [21]–[25] to support their C&CG customizations for two-stage RO problems dealing with flexible operation, multi-energy coordination, and the resilience issues in power systems.

Regardless that many studies assume and depend on the strong duality property of SOCP, we would like to highlight that the strong duality of an SOCP formulation does not hold in general, i.e., there may exist a non-zero gap between the primal and dual problems, as demonstrated in optimization literature (e.g., [26], [27]). In the context of power systems, our numerical studies (as in Section III and in Section V-B) actually reveal that the duality gap of some radial power networks could be non-negligible. For example, a 7.96% relative duality gap has been observed between the primal and dual SOCPs of AC OPF formulation for a real-world 56-bus distribution network.

Theoretically speaking, if the strong conic duality cannot be guaranteed, results obtained based on the dual of SOCP formulation can only be treated as heuristic ones. As demonstrated in our max-min bilevel optimization model with an SOCP based AC OPF in the lower level, the existence of duality gap has caused a 9.12% difference between the actual optimal value and the value derived by assuming strong duality. Accordingly, the worst case or contingency analysis result based on the strong duality assumption is misleading as it is not the actual one.

Hence, in this paper, to gain a deep understanding regarding SOCP power flow formulation and promote its applications, we present a study on its strong duality in radial power networks. Specifically, through a series of restrictive reformulations, we derive a set of closed form conditions (i.e., C1-C3) on network's physical parameters that guarantee the strong duality of the SOCP formulation for AC OPF model. These conditions can be verified prior to problem solving. Then, in our numerical studies on popular testing systems (including the IEEE test networks and two real-world distribution systems), we observe several instances that fail to have the strong duality. Nevertheless, when modified to satisfy the derived sufficient conditions, the strong conic duality of these OPF formulations can be achieved.

Our major contributions can be summarized as two-fold:

1) Through experiments on typical IEEE test beds and real world distribution systems, we numerically verify the existence of duality gaps between the primal and dual formulations of the SOCP-based OPF model. It indicates that, unless we can ensure the strong duality property, solutions derived based that dual formulation might not be exact. Actually, the gap can be significant.
2) We also theoretically derive a set of closed-form sufficient conditions (i.e., C1-C3) as well as a linear inequality system on network's physical parameters, which guarantees the strong duality of such SOCP formulation. We note that those sufficient conditions have been adopted for algorithm development in Refs [28]–[30], which justify the importance of our results.

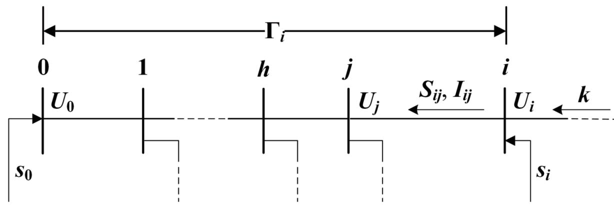

Fig. 1. Demonstration of Radial Power Network

The remainder of this paper is organized as below. Section II outlines the SOCP formulation for AC OPF model in radial networks. One simple example and one bilevel optimization example of that formulation are presented in Section III to demonstrate the impact of nonzero duality gaps. Section IV presents the theoretical derivations for our sufficient conditions. The derived conditions are numerically verified in Section V. Finally, conclusions are drawn in Section VI.

II. Conic AC Optimal Power Flow Model

Consider a power network with radial topology, i.e., a spanning tree network structure, as depicted in Fig. 1. We represent such a radial network as $(\mathcal{N}, \mathcal{E})$. Let $\mathcal{N} = \{0\} \cup \{\mathcal{N}^+\}$ denote the set of nodes such that the substation is node 0 and the rest nodes are $i = 1, 2, \ldots, n \in \mathcal{N}^+$. Because of the spanning tree structure with node 0 being the root, we denote the unique parent node of node i by j, and consequently, can identify the unique path from node 0 to i, which is denoted by Γ_i. Also, the children nodes of node i are denoted by k (through path $k \to i$). Let $\mathcal{E}$ denote the set of branches such that $(i, j) \in \mathcal{E}$. Since branch (i, j) is uniquely defined by node i, we use the indices i and (i, j) interchangeably in the rest of this paper.

In the following, we present a branch flow model (BFM) based AC OPF formulation as in (1)-(8). The objective function in (1) is to minimize the operational costs associated with the variables, e.g., nodal power generation and current flows. For this formulation, unless explicitly stated, the objective function f is convex without any special structure. Note that the basic form of this formulation (i.e., (1)-(8)) has been proposed in [31], [32] and many variants have been adopted for different applications, e.g., [12]–[15], [21]–[23].

$$\mathbf{OPF}: \quad \min \ f(\boldsymbol{\ell}, \boldsymbol{s}, \boldsymbol{v}, \boldsymbol{S}) \tag{1}$$

$$s.t. \ s_i = S_{ij} - \sum_{k:k\to i} (S_{ki} - z_{ki}\ell_{ki}), \quad \forall i \in \mathcal{N}^+ \tag{2}$$

$$s_0 = -\sum_{k:k\to 0} (S_{k0} - z_{k0}\ell_{k0}) \tag{3}$$

$$v_i - v_j = 2\mathrm{Re}(\bar{z}_{ij} S_{ij}) - |z_{ij}|^2 \ell_{ij}, \quad \forall (i,j) \in \mathcal{E} \tag{4}$$

$$\ell_{ij} = \frac{|S_{ij}|^2}{v_i}, \quad \forall (i,j) \in \mathcal{E} \tag{5}$$

$$0 \le \ell_{ij} \le \overline{\ell}_{ij}, \quad \forall (i,j) \in \mathcal{E} \tag{6}$$

$$\underline{v}_i \le v_i \le \overline{v}_i, \quad \forall i \in \mathcal{N}^+ \tag{7}$$

$$\underline{s}_i \le s_i \le \overline{s}_i, \quad \forall i \in \mathcal{N}^+ \tag{8}$$

Note that the **bold type** in (1) is to represent the vector of variables, e.g., $\boldsymbol{\ell} = \{\ell_{ij}\}_{(i,j)\in\mathcal{E}}$. Variable $\ell_{ij}(=I_{ij}^2)$ denotes the squared magnitude of current on branch $(i,j)\in\mathcal{E}$, which is bounded by a positive parameter $\overline{\ell}_{ij}(=\overline{I}_{ij}^2)$ as in (6). Variable $v_i(=U_i^2)$ denotes the squared magnitude of voltage at node $i\in\mathcal{N}^+$, whose upper and lower bounds are denoted by $\overline{v}_i(=\overline{U}_i^2)$ and $\underline{v}_i(=\underline{U}_i^2)$ as in (7). Variable $s_i = p_i + \mathbf{i}q_i$ is the power injection at node $i\in\mathcal{N}^+$, where p_i and q_i denote the active and reactive power injections. Similarly, $S_{ij} = P_{ij} + \mathbf{i}Q_{ij}$ is the power flow though branch $(i,j)\in\mathcal{E}$, where P_{ij} and Q_{ij} denote the active and reactive power flows. The connection between nodal power injections and power flows is defined by the branch flow equations (2)-(5). Parameter $z_{ij} = r_{ij} + \mathbf{i}x_{ij}$ is the impedance of branch $(i,j)\in\mathcal{E}$, where r_{ij} and x_{ij} denoting the line resistance and reactance. We also mention that the power injection at the substation node, i.e., node 0, are denoted by $s_0 = p_0 + \mathbf{i}q_0$, and the associated square of the reference voltage level is fixed to a constant $v_0(=U_0^2)$.

As mentioned in [9], the bounding for a complex variable applies to both its real and imaginary parts, e.g., $s < \overline{s}$ denotes $\mathrm{Re(s)} < \mathrm{Re(\overline{s})}$ and $\mathrm{Im(s)} < \mathrm{Im(\overline{s})}$. Accordingly, the upper and lower bounds of s_i are represented by $\overline{s}_i = \overline{p}_i + \mathbf{i}\overline{q}_i$ and $\underline{s}_i = \underline{p}_i + \mathbf{i}\underline{q}_i$ respectively as in (8). Note that parameters $(\underline{p}_i, \overline{p}_i, \underline{q}_i, \overline{q}_i)$ could be either positive or negative depending on the category of node i, e.g., the node that integrating distributed energy resources (DERs), Var compensators, or flexible loads [9].

Remark 1. *Due to the nonlinear equality constraint* (5)*, **OPF** in* (1)-(8) *is nonconvex. To convexify this formulation,* (5) *is relaxed to the following second-order conic inequality [7]–[9] (i.e., the rotated form):*

$$\ell_{ij} \geq \frac{|S_{ij}|^2}{v_i}, \quad \forall (i,j)\in\mathcal{E} \tag{9}$$

As a result, we obtain a convex relaxation of **OPF** *with affine and SOCP constraints, which includes* (1)-(4)*,* (6)-(8)*, and* (9)*. We denote this relaxation by **OPF-Cr**. In particular, if the objective function f is affine or convex quadratic, **OPF-Cr** is an SOCP formulation (denoted by **OPF-SOCP**), which, under some sufficient conditions [7]–[9], is exact and guarantees an optimal solution to the original **OPF** model.*

We mention that **OPF-SOCP** is computationally friendly and can be readily solved by a few commercial solvers, e.g., GUROBI, CPLEX, and MOSEK. Together with its stronger modeling accuracy over the classical linear programming based DC optimal power flow model, **OPF-SOCP** has been adopted to support many system design and operational studies, e.g., in [12]–[15], [21]–[23]. However, it probably does not have the strong duality property in general, which is very different from the classical LP based formulation. Next, we present two examples to illustrate the duality gap issue.

III. Nonzero Duality Gap of SOCP-Based Optimal Power Flow Formulation: Examples

A. Example 1: An SOCP Instance with Duality Gap

To demonstrate that nonzero duality gap could occur on **OPF-SOCP**, we consider the example of IEEE 33-bus distribution network, a popular test system adopted in many studies, e.g., [10], [19], [22], [23]. We consider an objective function f that minimizes the total network losses as in [31]–[33], i.e.,

TABLE I
Power Outputs of Nodal Devices: Exemplary System

Node	1	13	21	24	32
PV Panels	0	0.640MW	0.427MW	1.067MW	0.854MW
Var Generator	0.30Mvar	0.60Mvar	0.60Mvar	0.60Mvar	0.60Mvar

$$J_{\mathrm{p}} = \min \sum_{(i,j)\in\mathcal{E}} r_{ij}\ell_{ij} \tag{10}$$

Hence, the dual form of **OPF-SOCP** can be written as:

$$\begin{aligned} J_{\mathrm{d}} = \max & \sum_{i\in\mathcal{N}^+}(\overline{v}_i\gamma_i^u - \underline{v}_i\gamma_i^l) + \sum_{(i,j)\in\mathcal{E}}\overline{\ell}_{ij}\rho_{ij} \\ & + \sum_{i\in\mathcal{N}^+}\left(\overline{p}_i\phi_i^u - \underline{p}_i\phi_i^l + \overline{q}_i\varphi_i^u - \underline{q}_i\varphi_i^l\right) \end{aligned} \tag{11}$$

$$s.t.\ \pi_i + \phi_i^u - \phi_i^l = 0, \quad \forall i\in\mathcal{N}^+ \tag{12}$$

$$\tau_i + \varphi_i^u - \varphi_i^l = 0, \quad \forall i\in\mathcal{N}^+ \tag{13}$$

$$\pi_0 = 0 \tag{14}$$

$$\tau_0 = 0 \tag{15}$$

$$\pi_j - \pi_i - 2r_{ij}\theta_{ij} + \sigma_{ij} = 0, \quad \forall (i,j)\in\mathcal{E} \tag{16}$$

$$\tau_j - \tau_i - 2x_{ij}\theta_{ij} + \varsigma_{ij} = 0, \quad \forall (i,j)\in\mathcal{E} \tag{17}$$

$$\theta_{ij} - \sum_{k:k\to i}\theta_{ki} + \gamma_i^u - \gamma_i^l - \kappa_{ij} + \omega_{ij} \leq 0, \quad \forall i\in\mathcal{N}^+ \tag{18}$$

$$-\left(r_{ij}\pi_j + x_{ij}\tau_j\right) + \left(r_{ij}^2 + x_{ij}^2\right)\theta_{ij} + \rho_{ij} + \kappa_{ij} + \omega_{ij} \leq r_{ij}, \quad \forall (i,j)\in\mathcal{E} \tag{19}$$

$$\left\| \begin{matrix} \sigma_{ij} \\ \varsigma_{ij} \\ \kappa_{ij} \end{matrix} \right\|_2 \leq \omega_{ij}, \quad \forall (i,j)\in\mathcal{E} \tag{20}$$

where π_i, τ_i, π_0, τ_0, θ_{ij}, ρ_{ij}, (γ_i^l, γ_i^u), (ϕ_i^l, ϕ_i^u), and $(\varphi_i^l, \varphi_i^u)$ denote the dual variables associated with affine constraints (2)-(4) and (6)-(8), while σ_{ij}, ς_{ij}, κ_{ij}, and ω_{ij} are the dual variables of conic constraint (9). The detailed procedure to derive the dual **OPF-SOCP** can be found in Appendix A.

For the sake of illustration, we modify the standard 33-bus system by integrating photovoltaic (PV) panels and Var generators at node 1, 13, 21, 24, and 32 respectively. The nodal active/reactive power outputs are presented as in Table I. Also, we set $\underline{U}_i = 0.95U_0$ and $\overline{U}_i = 1.05U_0$, where $U_0 = 10$kV, and $\overline{I} = 250$A. Given such conditions, the primal and dual objectives of **OPF-SOCP** are optimized as $J_p = 1.188509$ and $J_d = 1.161750$ respectively. So, the absolute duality gap is

$$J_{\mathrm{p}} - J_{\mathrm{d}} = 1.188509 - 1.161750 = 0.026759\ \mathrm{MW},$$

and the relative duality gap is

$$\frac{J_{\mathrm{p}} - J_{\mathrm{d}}}{J_{\mathrm{p}}} = \frac{1.188509 - 1.161750}{1.188509} = 0.0225.$$

Note that this gap is much larger than the default optimality tolerance of our solver. Obviously, such significant gap is not due to that numerical tolerance. Hence, this instance fails to have the strong duality property.

B. Example 2: A Max-Min Bilevel Conic Optimization with Nonzero Duality Gap

To further investigate the impact of non-zero duality gap on real applications of SOCP-based AC OPF formulation, we consider a max-min extension embedding this formulation, i.e., a bilevel conic model based on (2)-(4), (6)-(9), and (10). Given a set of candidate siting sets over which PV units could be installed, we are evaluating their impact, under the worst case, on the network losses, which mathematically is expressed as:

$$\Gamma_{\text{bilevel}} = \max_{\boldsymbol{u}\in\mathcal{U}} \min_{(\boldsymbol{\ell},\boldsymbol{v},\boldsymbol{s},\boldsymbol{S})\in\Xi} \sum_{(i,j)\in\mathcal{E}} r_{ij}\ell_{ij} \tag{21}$$

$$s.t.\ \mathcal{U} = \left\{\boldsymbol{u}\in\{0,1\}^{|\mathcal{N}^+|} : \sum_{i\in\mathcal{N}^+} u_i \le K\right\} \tag{22}$$

$$\Xi = \{\boldsymbol{\ell},\boldsymbol{v},\boldsymbol{s},\boldsymbol{S}\in\mathbb{R}_+^m\times\mathbb{R}^n :\ (2)-(4),(6)-(9) \tag{23}$$

$$\overline{p}_i = \overline{p}_i^* + u_i\tilde{g}, \quad \forall i\in\mathcal{N}^+ \tag{24}$$

$$\underline{p}_i = \underline{p}_i^* + u_i\tilde{g}, \quad \forall i\in\mathcal{N}^+\} \tag{25}$$

where u_i is the binary indicator variable for PV siting status. The total number of integration sites is up to K. Note that the upper/lower bounds of nodal power injection are modified according to the PV siting status (in this instance, the energy curtailment is not allowed). Parameter $\tilde{g}$ denotes the real-time power generation of PV units.

If the strong duality holds, the bilevel optimization problem in (21)-(25) can be equivalently converted into a monolithic form by taking the dual of lower-level OPF problem. We have

$$\Gamma_{\text{single-level}} = \max \sum_{i\in\mathcal{N}^+}(\overline{v}_i\gamma_i^u - \underline{v}_i\gamma_i^l) + \sum_{(i,j)\in\mathcal{E}}\overline{\ell}_{ij}\rho_{ij}$$
$$+ \sum_{i\in\mathcal{N}^+}\left[\overline{p}_i^*\phi_i^u - \underline{p}_i^*\phi_i^l + \overline{q}_i^*\varphi_i^u - \underline{q}_i^*\varphi_i^l + \tilde{g}u_i\left(\phi_i^u - \phi_i^l\right)\right] \tag{26}$$

$$s.t.\ (12)-(20) \tag{27}$$

For this dual-SOCP based single-level equivalence in (26)-(27), considering the test conditions in Section III-A and setting $K = 1$ and $\tilde{g} = 53.35$KW, the professional solver GUROBI reports that the optimal value $\Gamma_{\text{single-level}}$ is 1.855702MW, and the PV unit is installed at node 20 (i.e., $u_{20} = 1$ while $u_{i|i\neq 20} = 0$).

Nevertheless, that optimal value is not the actual optimal value for the original bilevel optimization model. By enumerating all $i\in\mathcal{N}^+$ over the siting set $\mathcal{U}$ (which is finite and discrete) and directly computing the primal formulation in the lower level problem, we observe that the worst one (i.e., the highest one) is with $\Gamma_{\text{bilevel}} = 2.024936$MW, 9.12% larger than $\Gamma_{\text{single-level}}$. Clearly, the single-level reformulation fails to identify the worst PV integration site at node 22 (i.e., $u_{22} = 1$ while $u_{i|i\neq 22} = 0$).

Together with our observations in Section III-A, we can conclude that the strong duality does not hold in general for **OPF-SOCP**, and the duality gap could be nontrivial. As a direct consequence, unless the strong duality can be proven, computational methods relying on its dual formulation could lead to inexact or misleading solutions.

IV. Sufficient Conditions Ensuring Strong Duality

Before our theoretical derivation on sufficient conditions to ensure the strong duality of **OPF-Cr** (including **OPF-SOCP** as a special case), we first make a few rather non-restrictive assumptions:

- A1. The objective function f is bounded from below.
- A2. The bounds on squared magnitudes of voltages are strictly positive and they satisfy $\overline{v}_i > v_0 > \underline{v}_i > 0$ for all $i\in\mathcal{N}^+$. This is reasonable since they are practically set within a small deviation around v_0, e.g., $\underline{v}_i = (0.95)^2 v_0$, $\overline{v}_i = (1.05)^2 v_0$.
- A3. The line resistance and reactance are strictly positive, i.e., $r_{ij} > 0$ and $x_{ij} > 0$ for all $(i,j)\in\mathcal{E}$.

A. *OPF-Cr* Reformulations with Restrictions

To develop sufficient conditions on strong duality, we construct two auxiliary SOCPs by reformulating constraints in (2)-(4) and (6)-(9). First, by introducing new variables $\tau_{ij},\beta_{ij}\in\mathbb{R}$ for all $(i,j)\in\mathcal{E}$, we restrict our attention to a set of solutions of **OPF-Cr** (denoted by $\hat{\boldsymbol{S}},\hat{\boldsymbol{\ell}},\hat{\boldsymbol{s}},\hat{\boldsymbol{v}}$) that are represented as linear combinations of τ_{ij} and β_{ij}. Specifically,

$$\hat{S}_{ij} = \frac{z_{ij}(\tau_{ij}-\beta_{ij})}{|z_{ij}|^2}, \quad \forall(i,j)\in\mathcal{E} \tag{28}$$

$$\hat{\ell}_{ij} = \frac{\tau_{ij}}{|z_{ij}|^2}, \quad \forall(i,j)\in\mathcal{E} \tag{29}$$

Plugging (28)-(29) into equalities (2) and (3), variables $\hat{s}_i$ and $\hat{s_0}$ can be rewritten as

$$\hat{s}_i = \frac{z_{ij}}{|z_{ij}|^2}(\tau_{ij}-\beta_{ij}) + \sum_{k:k\to i}\frac{z_{ki}}{|z_{ki}|^2}\beta_{ki}, \quad \forall i\in\mathcal{N}^+ \tag{30}$$

$$\hat{s}_0 = \sum_{k:k\to 0}\frac{z_{k0}}{|z_{k0}|^2}\beta_{k0}. \tag{31}$$

Similarly, equality (4) can be converted into

$$\hat{v}_i - \hat{v}_j = \tau_{ij} - 2\beta_{ij}, \quad \forall(i,j)\in\mathcal{E}. \tag{32}$$

Moreover, because the nodal voltage $\hat{v}_i$ in (32) can be uniquely re-defined by summing the right-hand-side (RHS) expressions over the connected path Γ_i, $\hat{v}_i$ can be rewritten as

$$\hat{v}_i = v_0 + \sum_{(m,n)\in\Gamma_i}(\tau_{mn}-2\beta_{mn}), \quad \forall i\in\mathcal{N}^+. \tag{33}$$

In addition to (2)-(4), inequalities (6)-(9) should also be satisfied to ensure feasibility. Plugging (28)-(31) and (33) into conic constraint (9) and affine constraints (6)-(8), we have the first auxiliary SOCP (i.e., **OPF-SOCP**$_1$) as in (34)-(38).

$$v_0 + \sum_{(m,n)\in\Gamma_i}(\tau_{mn}-2\beta_{mn}) \ge \frac{(\tau_{ij}-\beta_{ij})^2}{\tau_{ij}}, \ \forall(i,j)\in\mathcal{E} \tag{34}$$

$$0 \le \tau_{ij} \le |z_{ij}|^2\overline{\ell}_{ij}, \quad \forall(i,j)\in\mathcal{E} \tag{35}$$

$$\underline{v}_i - v_0 \le \sum_{(m,n)\in\Gamma_i}(\tau_{mn}-2\beta_{mn}) \le \overline{v}_i - v_0, \quad \forall i\in\mathcal{N}^+ \tag{36}$$

$$\underline{p}_i \le \frac{r_{ij}}{|z_{ij}|^2}(\tau_{ij}-\beta_{ij}) + \sum_{k:k\to i}\frac{r_{ki}}{|z_{ki}|^2}\beta_{ki} \le \overline{p}_i, \quad \forall i\in\mathcal{N}^+ \tag{37}$$

$$\underline{q}_i \le \frac{x_{ij}}{|z_{ij}|^2}(\tau_{ij}-\beta_{ij}) + \sum_{k:k\to i}\frac{x_{ki}}{|z_{ki}|^2}\beta_{ki} \le \overline{q}_i, \quad \forall i\in\mathcal{N}^+ \tag{38}$$

Actually, by using the lower bound in (7) as well as assumption A2, we can derive a further restriction on inequality (34) (note that $\tau_{ij} \geq 0$ because of (35)) as in the following:

$$(\tau_{ij} - \beta_{ij})^2 \leq \underline{v}_i \tau_{ij}, \quad \forall (i,j) \in \mathcal{E} \tag{39}$$

With (39) being a conic inequality, our second auxiliary SOCP (i.e., **OPF-SOCP**$_2$) is defined by (35)-(38) and (39).

Remark 2. *As mentioned, auxiliary problems **OPF-SOCP**$_1$ and **OPF-SOCP**$_2$ define the restricted solution spaces of **OPF-Cr**. We also note that **OPF-SOCP**$_2$ is a restriction to **OPF-SOCP**$_1$. Hence, the feasible sets of **OPF-Cr**, **OPF-SOCP**$_1$ and **OPF-SOCP**$_2$ (denoted by $\mathbb{X}_{\text{OPF-Cr}}$, $\mathbb{X}_{\text{OPF-SOCP}_1}$ and $\mathbb{X}_{\text{OPF-SOCP}_2}$) satisfy the following relationship:*

$$\mathbb{X}_{\text{OPF-SOCP}_2} \subset \mathbb{X}_{\text{OPF-SOCP}_1} \subset \mathbb{X}_{\text{OPF-Cr}}. \tag{40}$$

*B. Strong Duality of Reformulations and **OPF-Cr***

Following *Slater's Condition*, the strong duality holds for a general SOCP problem if either its primal problem or dual problem is bounded and strictly feasible, i.e., the problem is feasible and all the non-affine (conic) inequality constraints hold with strict inequalities [34], [35]. Hence, the **OPF-Cr** and our auxiliary SOCPs, which are bounded because of assumption A1, have the strong duality as long as they are (essentially) strictly feasible. Next, we consider the strict feasibility of **OPF-SOCP**$_2$.

Lemma 1. ***OPF-SOCP**$_2$ is strictly feasible and thus has the strong duality if any of the following conditions is satisfied:*

- C1. *For every $i \in \mathcal{N}^+$, the bounds of its power injection satisfy either (i) $\underline{p}_i \leq 0 \leq \overline{p}_i$, $\underline{q}_i < 0 < \overline{q}_i$; or (ii) $\underline{p}_i < 0 < \overline{p}_i$, $\underline{q}_i \leq 0 \leq \overline{q}_i$; or (iii) $\underline{p}_i < 0 \leq \overline{p}_i$, $\underline{q}_i < 0 \leq \overline{q}_i$; or (iv) $\underline{p}_i \leq 0 < \overline{p}_i$, $\underline{q}_i \leq 0 < \overline{q}_i$.*
- C2. *$r_{ij}/x_{ij} \geq r_{ki}/x_{ki}$ for all $(i,j),(k,i) \in \mathcal{E}$; and $\underline{p}_i \leq 0 \leq \overline{p}_i$, $\underline{q}_i \leq 0 < \overline{q}_i$ for all $i \in \mathcal{N}^+$.*
- C3. *$r_{ij}/x_{ij} \leq r_{ki}/x_{ki}$ for all $(i,j),(k,i) \in \mathcal{E}$; and $\underline{p}_i \leq 0 < \overline{p}_i$, $\underline{q}_i \leq 0 \leq \overline{q}_i$ for all $i \in \mathcal{N}^+$.*

Proof. *We make use of two new variables $\mu \in \mathbb{R}_+$ and $\lambda_{ij} \in \mathbb{R}$ to simplify the constraints over τ_{ij} and β_{ij} for all $(i,j) \in \mathcal{E}$. Specifically, we have*

$$\tau_{ij} = \frac{|z_{ij}|^2 \overline{\ell}_{ij}}{\mu}, \quad \forall (i,j) \in \mathcal{E} \tag{41}$$

$$\beta_{ij} = \lambda_{ij} \tau_{ij}, \quad \forall (i,j) \in \mathcal{E} \tag{42}$$

Because of inequality (35), we have $\mu \geq 1$. Then, plugging (41) and (42) into the strict version of inequality of (39) as well as affine inequalities (36)-(38), we have

$$\frac{(1-\lambda_{ij})^2}{\mu} < \frac{\underline{v}_i}{|z_{ij}|^2 \overline{\ell}_{ij}}, \quad \forall (i,j) \in \mathcal{E} \tag{43}$$

$$\underline{v}_i - v_0 \leq \sum_{(m,n)\in\Gamma_i} |z_{mn}|^2 \overline{\ell}_{mn} \frac{1-2\lambda_{mn}}{\mu} \leq \overline{v}_i - v_0, \quad \forall i \in \mathcal{N}^+ \tag{44}$$

$$\underline{p}_i \leq r_{ij}\overline{\ell}_{ij}\frac{1-\lambda_{ij}}{\mu} + \frac{1}{\mu}\sum_{k:k\to i} r_{ki}\overline{\ell}_{ki}\lambda_{ki} \leq \overline{p}_i, \quad \forall i \in \mathcal{N}^+ \tag{45}$$

$$\underline{q}_i \leq x_{ij}\overline{\ell}_{ij}\frac{1-\lambda_{ij}}{\mu} + \frac{1}{\mu}\sum_{k:k\to i} x_{ki}\overline{\ell}_{ki}\lambda_{ki} \leq \overline{q}_i, \quad \forall i \in \mathcal{N}^+ \tag{46}$$

Clearly, with a finite λ_{ij} and $\mu \to +\infty$, the strict inequality in (43) can be easily achieved given that the left-hand-side of (43) approaches to 0+ while its RHS is a positive constant following assumptions A2-A3. Also, through assumption A2, we have $\underline{v}_i - v_0 < 0 < \overline{v}_i - v_0$. When $\mu \to +\infty$, inequality (44) holds as its middle term approaches to 0.

Similarly, the feasibility of inequalities (45) and (46) can be ensured by properly setting the bounds of power injections, i.e., $\overline{p}_i/\underline{p}_i$ and $\overline{q}_i/\underline{q}_i$. let $\delta^p_{ij}, \delta^q_{ij} \in \mathbb{R}$ be such that

$$\delta^p_{ij} = 1 - \lambda_{ij} + \frac{\sum_{k:k\to i} \lambda_{ki} r_{ki} \overline{\ell}_{ki}}{r_{ij}\overline{\ell}_{ij}}, \quad \forall (i,j) \in \mathcal{E} \tag{47}$$

$$\delta^q_{ij} = 1 - \lambda_{ij} + \frac{\sum_{k:k\to i} \lambda_{ki} x_{ki} \overline{\ell}_{ki}}{x_{ij}\overline{\ell}_{ij}}, \quad \forall (i,j) \in \mathcal{E} \tag{48}$$

Accordingly, inequalities (45) and (46) are equivalent to:

$$\underline{p}_i \leq \frac{r_{ij}\overline{\ell}_{ij}\delta^p_{ij}}{\mu} \leq \overline{p}_i, \quad \forall i \in \mathcal{N}^+ \tag{49}$$

$$\underline{q}_i \leq \frac{x_{ij}\overline{\ell}_{ij}\delta^q_{ij}}{\mu} \leq \overline{q}_i, \quad \forall i \in \mathcal{N}^+ \tag{50}$$

Note that if $\delta^p_{ij} = 0$ (or $\delta^q_{ij} = 0$), the middle term of (49) or (50) will be zero so that it requires $\underline{p}_i \leq 0 \leq \overline{p}_i$ (or $\underline{q}_i \leq 0 \leq \overline{q}_i$) to ensure its feasibility; if $\delta^p_{ij} < 0$ (or $\delta^q_{ij} < 0$) and let $\mu \to +\infty$, the middle term of (49) or (50) will approach to 0−, which requires $\underline{p}_i < 0 \leq \overline{p}_i$ (or $\underline{q}_i < 0 \leq \overline{q}_i$) to ensure its feasibility; if $\delta^p_{ij} > 0$ (or $\delta^q_{ij} > 0$), it requires $\underline{p}_i \leq 0 < \overline{p}_i$ (or $\underline{q}_i \leq 0 < \overline{q}_i$) to ensure its feasibility. For undetermined δ^p_{ij} and δ^q_{ij}, constraints (49)-(50) are feasible as long as $\underline{p}_i < 0 < \overline{p}_i$ and $\underline{q}_i < 0 < \overline{q}_i$.

*Considering the spanning tree structure of $(\mathcal{N}, \mathcal{E})$, λ_{ki} corresponds to the downstream branches of node i, while λ_{ij} corresponds to its unique upstream branch. Hence, for a group of λ_{ki} with arbitrary values, either δ^p_{ij} or δ^q_{ij} can be specified by picking up a proper λ_{ij}, and then it dominates the value of the other. So we can always find a λ_{ij} to satisfy either (a) $\delta^p_{ij} = 0$, or (b) $\delta^q_{ij} = 0$, or (c) $\max\{\delta^p_{ij}, \delta^q_{ij}\} \leq 0$, or (d) $\min\{\delta^p_{ij}, \delta^q_{ij}\} \geq 0$ for every $(i,j) \in \mathcal{E}$, which corresponds to (i)-(iv) in condition **C1** that ensure the strict feasibility and thus the strong duality of **OPF-SOCP**$_2$.*

*Moreover, some alternative conditions of **C1** can be derived under special network parameters. For instance, if $r_{ij}/x_{ij} \geq r_{ki}/x_{ki}$ and let $\lambda_{ij} > 0$ for all $(i,j),(k,i) \in \mathcal{E}$, then we have*

$$\frac{r_{ij}}{x_{ij}} \geq \frac{r_{ki}}{x_{ki}} \Leftrightarrow \frac{\sum_{k:k\to i} \lambda_{ki} r_{ki}\overline{\ell}_{ki}}{\sum_{k:k\to i} \lambda_{ki} x_{ki}\overline{\ell}_{ki}} \cdot \frac{x_{ij}\overline{\ell}_{ij}}{r_{ij}\overline{\ell}_{ij}} \leq 1$$
$$\Leftrightarrow \frac{\sum_{k:k\to i} \lambda_{ki} r_{ki}\overline{\ell}_{ki}}{r_{ij}\overline{\ell}_{ij}} \leq \frac{\sum_{k:k\to i} \lambda_{ki} x_{ki}\overline{\ell}_{ki}}{x_{ij}\overline{\ell}_{ij}} \Leftrightarrow \delta^p_{ij} \leq \delta^q_{ij} \tag{51}$$

*Hence, there always exists a $\lambda_{ij} \in \mathbb{R}_+$ for every $(i,j) \in \mathcal{E}$ such that $\delta^q_{ij} \geq \delta^p_{ij} = 0$. Then, it requires $\underline{p}_i \leq 0 \leq \overline{p}_i$, $\underline{q}_i \leq 0 < \overline{q}_i$ as in **C2** to guarantee the strong duality of **OPF-SOCP**$_2$.*

*Similarly, when $r_{ij}/x_{ij} \leq r_{ki}/x_{ki}$, there exits a $\lambda_{ij} \in \mathbb{R}_+$ for every $(i,j) \in \mathcal{E}$ such that $\delta^p_{ij} \geq \delta^q_{ij} = 0$, which requires $\underline{p}_i \leq 0 < \overline{p}_i$, $\underline{q}_i \leq 0 \leq \overline{q}_i$ as in **C3** to ensure the strong duality. This completes the proof.* ■

Based on Lemma 1, and the relationship among **OPF-SOCP**$_2$, **OPF-SOCP**$_1$ and **OPF-Cr** (including the special case **OPF-SOCP**) stated in Remark 2, we have:

Theorem 1. ***OPF-SOCP***$_1$ *and* ***OPF-Cr*** *are strictly feasible and thus have the strong duality when either of the conditions C1-C3 is satisfied.*

Corollary 1. *The strong duality of* ***OPF-SOCP*** *holds when either of the conditions C1-C3 is satisfied.*

Additionally, by using (43) and $\mu \geq 1$, we derive another extension of auxiliary SOCP (43)-(46), which is to generalize a linear inequality system (denoted by **LIS**) as follows:

$$|1 - \lambda_{ij}| \leq \sqrt{\frac{\tilde{v}_i}{|z_{ij}|^2 \overline{\ell}_{ij}}}, \quad \forall (i,j) \in \mathcal{E} \tag{52}$$

$$(\underline{v}_i - v_0)\mu \leq \sum_{(m,n)\in\Gamma_i} |z_{mn}|^2 \overline{\ell}_{mn}(1 - 2\lambda_{mn}) \leq (\overline{v}_i - v_0)\mu, \quad \forall i \in \mathcal{N}^+ \tag{53}$$

$$\underline{p}_i \mu \leq r_{ij}\overline{\ell}_{ij}(1 - \lambda_{ij}) + \sum_{k:k\to i} r_{ki}\overline{\ell}_{ki}\lambda_{ki} \leq \overline{p}_i \mu, \ \forall i \in \mathcal{N}^+ \tag{54}$$

$$\underline{q}_i \mu \leq x_{ij}\overline{\ell}_{ij}(1 - \lambda_{ij}) + \sum_{k:k\to i} x_{ki}\overline{\ell}_{ki}\lambda_{ki} \leq \overline{q}_i \mu, \ \forall i \in \mathcal{N}^+ \tag{55}$$

$$\mu \geq 1 \tag{56}$$

Let $\tilde{v}_i = \underline{v}_i - \varepsilon$, where ε is a sufficiently small and positive number. Clearly, **LIS** is a restriction to (43)-(46) as well as **OPF-SOCP**$_2$. Denote the feasible set of **LIS** as $\mathbb{X}_{\mathrm{LIS}}$ and together with (40), we have

$$\mathbb{X}_{\mathrm{LIS}} \subset \mathbb{X}_{\mathrm{OPF-SOCP_2}} \subset \mathbb{X}_{\mathrm{OPF-SOCP_1}} \subset \mathbb{X}_{\mathrm{OPF-Cr}} \tag{57}$$

As implied by (57), the feasibility of (52)-(56) ensures the strict feasibility and thus the strong duality of **OPF-Cr**.

Corollary 2. *The strong duality of* ***OPF-SOCP*** *holds when the linear inequality system* (52)-(56) *is feasible.*

Remark 3. *Note that the feasibility of* ***LIS*** *only depends on the input parameters of an OPF problem, which can be readily checked to identify the instances that have the strong duality.*

C. A Special OPF-SOCP Formulation with Strong Duality

In practical situations, the nodal power injection is usually expressed as $s_i = s_i^g - \tilde{s}_i^d$, where s_i^g and $\tilde{s}_i^d$ denote the adjustable generation (i.e., a complex variable) and load demand (i.e., a nonnegative constant) at node $i \in \mathcal{N}^+$. Moreover, if the load curtailment (denoted by $s_i^c = p_i^c + \mathbf{i} q_i^c$) is allowed, **OPF-Cr** can be modified as:

$$\mathbf{MOPF-Cr}: \ \min \ f(\boldsymbol{\ell}, \boldsymbol{s}^g, \boldsymbol{v}) + h(\boldsymbol{s}^c) \tag{58}$$

$$s.t. \ s_i = s_i^g - (\tilde{s}_i^d - s_i^c), \quad \forall i \in \mathcal{N}^+ \tag{59}$$

$$\underline{p}_i^g \leq \mathrm{Re}(s_i^g) \leq \overline{p}_i^g, \ \underline{q}_i^g \leq \mathrm{Im}(s_i^g) \leq \overline{q}_i^g, \quad \forall i \in \mathcal{N}^+ \tag{60}$$

$$0 \leq \mathrm{Re}(s_i^c) \leq \overline{p}_i^c, \ 0 \leq \mathrm{Im}(s_i^c) \leq \overline{q}_i^c, \quad \forall i \in \mathcal{N}^+ \tag{61}$$

$$\text{Eqs. } (2)-(4),(6),(7),(9) \tag{62}$$

where h is the convex penalty function on curtailment variable $\boldsymbol{s}^c$, whose real and imaginary parts are restricted by upper bounds $\overline{p}_i^c$ and $\overline{q}_i^c$ respectively. Moreover, the upper and lower bounds of nodal generation are represented by $\overline{p}_i^g/\underline{p}_i^g$ and $\overline{q}_i^g/\underline{q}_i^g$ respectively. Following the ideas in Ref [9], the boundaries of reactive power generation can be defined as:

$$\overline{q}_i^g = \tilde{z}_i^v q_i^{v,\max}, \ \underline{q}_i^g = 0, \quad \forall i \in \mathcal{N}^+ \tag{63}$$

where parameters $q_i^{v,\max}$ and $\tilde{z}_i^v$ denote the rated capacity and the commitment status of Var compensators (e.g., the shunt capacitors [9]) at node i.

Also, without loss of generality, we have

$$\overline{p}_i^g = \tilde{z}_i^g p_i^{g,\max}, \ \underline{p}_i^g = \tilde{z}_i^g p_i^{g,\min}, \quad \forall i \in \mathcal{N}^+ \tag{64}$$

where $p_i^{g,\max}$ and $p_i^{g,\min}$ denote the rated capacity and minimum output of active power generators, while $\tilde{z}_i^g$ is a prespecified parameter that describes their availability status. Note that $\tilde{z}_i^g = 0$ indicates that the generating units are offline (or not deployed) such that $\overline{p}_i^g = \underline{p}_i^g = 0$. Otherwise, when $\tilde{z}_i^g = 1$, the nodal generation will be activated, then we have $\overline{p}_i^g \geq \underline{p}_i^g \geq 0$.

Corollary 3. *The strong duality of* ***MOPF-Cr*** *holds if (i) the upper bounds of load curtailment variable* $\boldsymbol{s}^c$ *are positive and sufficiently large, and (ii) for every* $i \in \mathcal{N}^+$*, either* $\tilde{z}_i^g = 0$ *or* $p_i^{g,\min} \leq \mathrm{Re}(\tilde{s}_i^d)$.

Proof. *Because of* (59)-(64)*, the nodal injection variable* s_i *satisfies* (65)-(66) *for all* $i \in \mathcal{N}^+$*:*

$$\tilde{z}_i^g p_i^{g,\min} - \mathrm{Re}(\tilde{s}_i^d) \leq \mathrm{Re}(s_i) \leq \tilde{z}_i^g p_i^{g,\max} + \overline{p}_i^c - \mathrm{Re}(\tilde{s}_i^d) \tag{65}$$

$$-\mathrm{Im}(\tilde{s}_i^d) \leq \mathrm{Im}(s_i) \leq \tilde{z}_i^v q_i^{v,\max} + \overline{q}_i^c - \mathrm{Im}(\tilde{s}_i^d) \tag{66}$$

Clearly, we have $\overline{p}_i, \overline{q}_i > 0$ *if* $\overline{p}_i^c$ *and* $\overline{q}_i^c$ *are sufficiently large. We also have* $\underline{q}_i = -\mathrm{Im}(\tilde{s}_i^d) \leq 0$ *based on* (63)*. Moreover, the second statement in Corollary 3 deduces* $\tilde{z}_i^g p_i^{g,\min} - \mathrm{Re}(\tilde{s}_i^d) \leq 0$*. Thus it follows condition C1-(iv) that* (58)-(62) *is strictly feasible, which ensures the strong duality of* ***MOPF-Cr****.* ■

Remark 4. *Note that a large bound could rarely lead to irrational load curtailment (i.e., the amount of curtailment exceeds the nominal load capacity) whenever* ***MOPF-Cr*** *achieves its global optimum. That is because: (a) the penalty factor for load curtailment is usually very large; (b) a unified penalty factor is typically applied for every node. Furthermore, if the objective function* (1) *is affine or convex quadratic while both conditions in Corollary 3 can be satisfied, we denote this version of* ***MOPF-Cr*** *as* ***MOPF-SOCP****.*

Corollary 4. *The modified OPF formulation in* ***MOPF-SOCP*** *has the strong duality.*

V. Numerical Verification

Numerical evaluations are conducted on IEEE 33-bus, 69-bus test networks and SCE 47-, 56-bus networks (i.e., two real-world distribution systems served by the Southern California Edison (SCE) company). We aim to verify that: 1) non-negligible duality gaps exist in the standard SOCP formulations for AC OPF in both the test networks and real-world systems; and 2) the modifications based on the proposed sufficient conditions C1-C3 lead to the strong conic duality.

A. Test Systems

Similar to those in Section III, the test distribution networks (originally without power sources) are upgraded by adding the PV panels and shunt capacitors (or static Var generators) as active and reactive power sources. Fig. 2 presents the modified system structures of IEEE 33-bus and 69-bus networks.

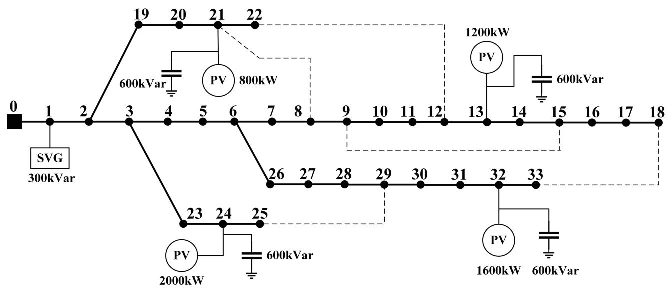

(a) IEEE 33-Bus Network

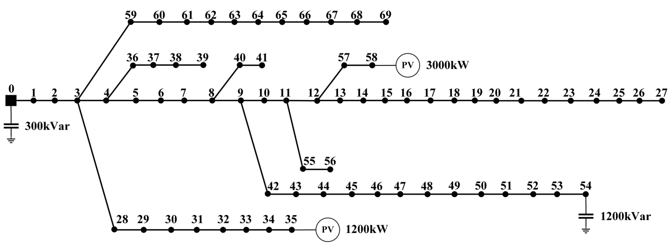

(b) 69-Bus Network

Fig. 2. Test Radial Power Networks

Detailed network parameters are available in [36]. Also, the parameters of SCE distribution systems can be referred to [9]. Note that the variability of PV generation and load profiles are represented by a large set of scenarios (including more than 12,000 instances). Following the ideas in Ref [37], the random scenarios are produced using Latin Hypercube sampling (LHS) technique based on the historical solar and load profiles. By fitting the sampling data into (65)-(66), we derive a cluster of power boundary parameters, i.e., $[\underline{p}_i, \overline{p}_i]$ and $[\underline{q}_i, \overline{q}_i]$.

Additionally, we mention that every OPF models (including their primal and dual forms) are computed by GUROBI with an optimality tolerance for termination as 1.00E-04 and the time restriction to 600 seconds. All experiments are performed in the MATLAB environment on a personal computer with Intel Core i7-7820HQ 2.90GHZ processor and 32GB RAM.

B. Existence of Duality Gaps

The primal/dual **OPF-SOCP**s of the IEEE test networks and SCE systems are computed to derive the relative duality gaps. Table II presents the results of strong duality test under different instances of PV outputs and load demands. The average gaps and the maximum gaps are recorded in columns "Avg-G" and "G^+" respectively. Let ϵ denote the acceptable relative gap for strong duality, which means that the instance with a relative duality gap less than ϵ can be considered to hold the strong duality. Then, we record the number and ratio of instances that fail the strong duality test (i.e., weak duality instances) in columns "N_WD" and "R_WD" with respect to different acceptable relative gap, i.e., $\epsilon = 1\%$, $\epsilon = 0.1\%$, and $\epsilon = 0.01\%$. Correspondingly, the ratio of instances that have the strong duality is given in column "R_SD". In addition, we record the average run time (as in column Avg-T) and the maximum run time (as in column T^+) to validate the solution status. The solution time is counted in seconds (secs).

As can be seen from Table II, all instances are computed to optimality within the time limit of 600 secs. The average time and the maximum time to compute the **OPF-SOCP** of original systems are 8.63 secs and 63.27 secs (as reported by a 69-bus test instance) respectively. That means, the difference between the actual global optimal solution and the solution reported by GUROBI is no more than 1.00E-4. Nevertheless, we observe the non-negligible duality gaps (i.e., larger than pre-specified gap tolerance) in the results of almost all test systems. The largest duality gap occurs in some instance of SCE 56-bus system and reaches 7.96%. So, such a large gap clearly cannot be attributed to numerical error or computational time restriction, and therefore fails the strong duality test.

Next, we discuss our test results in details.

1) When $\epsilon = 1\%$, although we can claim that most instances have the strong duality, there still exist 20 out of 12,765 instances failing our test. The worst case occurs on the SCE 56-bus system, where 0.45% of the instances report a duality gap larger than 1%.
2) When $\epsilon = 0.1\%$, the number of instances that fail our test has significantly increased from 20 to 206. Correspondingly, the ratio of strong duality instances drops. For example, when $\epsilon = 1\%$, all of the instances in 69-bus network can be claimed to have the strong duality. This ratio decreases to 98.07% when $\epsilon = 0.1\%$. Similar observations can be obtained from the results of other three test systems.
3) When $\epsilon = 0.01\%$, the number of instances that fail our test has reached 423. Indeed, more than 2.40% of the instances of 33-bus, 69-bus, and 56-bus distribution networks are observed to have a duality gap larger than 0.01%. By applying such standard, there will be 8.65% of the weak duality instances for SCE 47-bus system. The dual solution of these instances may not be applicable for practical use.

Overall, 3.31% of all instances in test systems demonstrate a duality gap larger than 0.01%, which is a nontrivial proportion. Hence, we may conclude that the strong duality property does not hold in general for the **OPF-SOCP** formulation.

C. Verification of Conditions C1-C3

The proposed conditions C1-C3 can be satisfied through the following strategies:

1) **Strategy for C1**: By using the strategy in Section IV-C, **MOPF-SOCP** is adopted to satisfy C1.
2) **Strategy for C2**: The first part of C2 can be satisfied by adjusting the physical parameters of radial network (i.e., modifying either the resistance or the reactance to make their ratios non-increasing along the paths from the root node to leaf nodes), while its second part requires for a sufficiently large bound on reactive load curtailment.
3) **Strategy for C3**: The realization of C3 is similar to C2 except that the bound on active load curtailment should be very large, while the ratios of resistance to reactance are required to be non-decreasing along the paths from the root node to leaf nodes.

TABLE II
STRONG DUALITY TEST ON ORIGINAL SYSTEMS

Test Systems	Avg-G	G$^+$	1.00%			0.10%			0.01%			Avg-T	T$^+$
			N_WD	R_WD	R_SD	N_WD	R_WD	R_SD	N_WD	R_WD	R_SD	/sec	/sec
IEEE 33-Bus	0.0026	0.0396	4	0.13%	99.87%	29	0.93%	99.07%	80	2.57%	97.43%	1.67	2.02
69-Bus Network	0.0019	0.0049	0	0	100.00%	100	1.93%	98.07%	129	2.49%	97.51%	18.96	63.27
SCE 47-Bus	0.0014	0.0176	3	0.19%	99.81%	38	2.45%	97.55%	134	8.65%	91.35%	1.84	29.70
SCE 56-Bus	0.0056	0.0796	13	0.45%	99.55%	39	1.34%	98.66%	80	2.75%	97.25%	1.28	1.47

TABLE III
STRONG DUALITY TEST ON MODIFIED SYSTEMS

Test Conditions		Avg-G	G$^+$	R_WD	R_SD	Avg-T/sec	T$^+$/sec
IEEE 33-Bus	Modified by C1	1.688E-06	5.182E-05	0%	100.0%	2.47	7.11
	Modified by C2	3.923E-07	1.294E-06	0%	100.0%	2.42	7.17
	Modified by C3	4.627E-07	3.616E-06	0%	100.0%	2.43	7.14
69-Bus Network	Modified by C1	1.956E-06	2.475E-05	0%	100.0%	25.89	63.86
	Modified by C2	1.627E-06	3.869E-06	0%	100.0%	2.29	3.88
	Modified by C3	7.689E-06	2.684E-05	0%	100.0%	2.30	3.80
SCE 47-Bus	Modified by C1	8.366E-06	9.606E-05	0%	100.0%	1.69	19.19
	Modified by C2	8.022E-07	2.268E-06	0%	100.0%	1.35	2.25
	Modified by C3	5.706E-07	3.499E-06	0%	100.0%	1.36	3.44
SCE 56-Bus	Modified by C1	4.474E-07	2.111E-06	0%	100.0%	1.30	3.77
	Modified by C2	8.927E-07	2.927E-06	0%	100.0%	1.27	2.11
	Modified by C3	4.900E-07	1.667E-06	0%	100.0%	1.31	3.64

The aforementioned strategies are applied to modify our test systems, and their primal and dual instances are computed to optimality as presented in Table III. Also, if we assume that the strong duality holds if the relative gap between optimal values of the primal and dual problems is less than or equal to 0.01% (i.e., $\epsilon = 0.01\%$), we report the proportions of weak-duality and strong-duality instances in columns "R_WD" and "R_SD" respectively.

As indicated by Table III, the computation time for modified **OPF-SOCP**s is comparable to the original ones. The average time and the maximum time to solve the OPF problem of modified systems are 5.20 secs and 63.86 secs respectively. Hence, those modified instances can be easily computed to optimality. Also, their duality gap are less than 1.00E-4 (mostly below 1.00E-5). For instances of the 56-bus system, which have the largest duality gap, their modified instances are with a maximum duality gap as 2.927E-06. It is reduced by orders of magnitude. The aforementioned results thus support our derivation on those sufficient conditions as the optimal value difference between the primal and dual problems are numerically negligible.

VI. CONCLUSION

This paper has demonstrated that the popular SOCP formulation for AC OPF in a radial network does not have the strong duality property in general. Nevertheless, it is proved that the strong duality holds if either of conditions C1-C3 can be met. In particular, some of these sufficient conditions can be easily satisfied through minor modifications. In addition to theoretical reasoning, our numerical studies confirm that non-negligible duality gaps *do exist* in SOCP formulations for AC OPF of IEEE 33-bus, 69-bus test networks and two real-world distribution systems. By applying some modifications based on C1-C3 in those systems, we then observe the strong duality in all of their test instances, which validates our proposed sufficient conditions. We expect that the presented results provide a substantial support to many SOCP related AC OPF studies, and pave the way to address the strong duality issue in other network structures.

APPENDIX A
DERIVATION OF DUAL **OPF-SOCP** PROBLEM

The dual formulation of **OPF-SOCP** can be derived through the following procedure.

1) Step 1: We first reformulate constraints (2)-(4), (6)-(8), and (9) to a group of real-valued inequalities. Let $s_i = p_i + \mathbf{i}q_i$, $S_{ij} = P_{ij} + \mathbf{i}Q_{ij}$, $z_{ij} = r_{ij} + \mathbf{i}x_{ij}$, which separate all those complex-form constraints, the primal **OPF-SOCP** can thus be rewritten as:

$$\mathbf{OPF-SOCP}: \; J_{\mathrm{p}} = \min \sum_{(i,j)\in\mathcal{E}} r_{ij}\ell_{ij} \tag{67}$$

$$s.t.\; p_i = P_{ij} - \sum_{k:k\to i}(P_{ki} - r_{ki}\ell_{ki}), \quad \forall i \in \mathcal{N}^+ \tag{68}$$

$$q_i = Q_{ij} - \sum_{k:k\to i}(Q_{ki} - x_{ki}\ell_{ki}), \quad \forall i \in \mathcal{N}^+ \tag{69}$$

$$p_0 = -\sum_{k:k\to 0}(P_{k0} - r_{k0}\ell_{k0}) \tag{70}$$

$$q_0 = -\sum_{k:k\to 0}(Q_{k0} - x_{k0}\ell_{k0}) \tag{71}$$

$$v_i - v_j = 2(r_{ij}P_{ij} + x_{ij}Q_{ij}) - (r_{ij}^2 + x_{ij}^2)\ell_{ij}, \forall (i,j)\in\mathcal{E} \tag{72}$$

$$0 \le \ell_{ij} \le \overline{\ell}_{ij}, \quad \forall (i,j)\in\mathcal{E} \tag{73}$$

$$\underline{v}_i \le v_i \le \overline{v}_i, \quad \forall i \in \mathcal{N}^+ \tag{74}$$

$$\underline{p}_i \le p_i \le \overline{p}_i, \quad \forall i \in \mathcal{N}^+ \tag{75}$$

$$\underline{q}_i \le q_i \le \overline{q}_i, \quad \forall i \in \mathcal{N}^+ \tag{76}$$

$$\left\| \begin{matrix} 2P_{ij} \\ 2Q_{ij} \\ \ell_{ij} - v_i \end{matrix} \right\|_2 \le \ell_{ij} + v_i, \quad \forall (i,j) \in \mathcal{E} \tag{77}$$

where (77) is the standard form of SOCP constraint (9). Let $\boldsymbol{Y}_{ij} = \begin{bmatrix} Y_{ij}^a & Y_{ij}^b & Y_{ij}^c \end{bmatrix}^T = \begin{bmatrix} 2P_{ij} & 2Q_{ij} & \ell_{ij} - v_i \end{bmatrix}^T$ and $y_{ij} = \ell_{ij} + v_i$ for all $(i,j) \in \mathcal{E}$, the conic inequality (77) can be equivalently expressed as the following constraints:

$$\left\| \boldsymbol{Y}_{ij} \right\|_2 \le y_{ij}, \quad \forall (i,j) \in \mathcal{E} \tag{78}$$

$$Y_{ij}^a = 2P_{ij}, \quad \forall (i,j) \in \mathcal{E} \tag{79}$$

$$Y_{ij}^b = 2Q_{ij}, \quad \forall (i,j) \in \mathcal{E} \tag{80}$$

$$Y_{ij}^c = \ell_{ij} - v_i, \quad \forall (i,j) \in \mathcal{E} \tag{81}$$

$$y_{ij} = \ell_{ij} + v_i, \quad \forall (i,j) \in \mathcal{E} \tag{82}$$

where Y_{ij}^a, Y_{ij}^b, and Y_{ij}^c denote the components of vector $\boldsymbol{Y}_{ij}$.

2) Step 2: Let π_i, τ_i, π_0, τ_0, θ_{ij}, ρ_{ij}, (γ_i^l, γ_i^u), (ϕ_i^l, ϕ_i^u), $(\varphi_i^l, \varphi_i^u)$, α_{ij}, σ_{ij}, ς_{ij}, κ_{ij}, and ω_{ij} denote the dual variables associated with constraints (68)-(76) and (78)-(82), we develop the Lagrangian function (i.e., $\mathcal{L}$) for **OPF-SOCP** and reorganize it with respect to the primal variables:

$$\begin{aligned}
\inf_{\boldsymbol{p},\boldsymbol{q},\boldsymbol{P},\boldsymbol{Q},\boldsymbol{v},\boldsymbol{\ell}} \mathcal{L} = \min & \sum_{i\in\mathcal{N}^+} \left(\overline{v}_i \gamma_i^u - \underline{v}_i \gamma_i^l\right) + \sum_{(i,j)\in\mathcal{E}} \overline{\ell}_{ij} \rho_{ij} \\
& + \sum_{i\in\mathcal{N}^+} \left(\overline{p}_i \phi_i^u - \underline{p}_i \phi_i^l + \overline{q}_i \varphi_i^u - \underline{q}_i \varphi_i^l \right) \\
& + \sum_{i\in\mathcal{N}^+} \left[p_i \left(-\pi_i + \phi_i^l - \phi_i^u\right) + q_i \left(-\tau_i + \varphi_i^l - \varphi_i^u\right) \right] \\
& + p_0(-\pi_0) + q_0(-\pi_0) \\
& + \sum_{(i,j)\in\mathcal{E}} P_{ij} \left(\pi_i - \pi_j + 2r_{ij}\theta_{ij} - \sigma_{ij}\right) \\
& + \sum_{(i,j)\in\mathcal{E}} Q_{ij} \left(\tau_i - \tau_j + 2x_{ij}\theta_{ij} - \varsigma_{ij}\right) \\
& + \sum_{i\in\mathcal{N}^+} v_i \left(-\theta_{ij} + \sum_{k:k\to i} \theta_{ki} + \gamma_i^l - \gamma_i^u + \kappa_{ij} - \omega_{ij} \right) \\
& + \sum_{(i,j)\in\mathcal{E}} \ell_{ij} [r_{ij} + r_{ij}\pi_j + x_{ij}\tau_j - (r_{ij}^2 + x_{ij}^2)\theta_{ij} \\
& \qquad - \rho_{ij} - \kappa_{ij} - \omega_{ij}] \\
& + \sum_{(i,j)\in\mathcal{E}} y_{ij} \left(\omega_{ij} - \alpha_{ij}\right) \\
& + \sum_{(i,j)\in\mathcal{E}} \left(\alpha_{ij} \left\| \boldsymbol{Y}_{ij} \right\|_2 + \boldsymbol{\nu}_{ij}^T \boldsymbol{Y}_{ij} \right)
\end{aligned} \tag{83}$$

where we define a vector $\boldsymbol{\nu}$ that is composed of dual variables corresponding to (79)-(81), such that

$$\boldsymbol{\nu}_{ij} = \begin{bmatrix} \sigma_{ij} & \varsigma_{ij} & \kappa_{ij} \end{bmatrix}^T, \quad \forall (i,j) \in \mathcal{E} \tag{84}$$

3) Step 3: An essential step of constructing the dual form of **OPF-SOCP** is to minimize the Lagrangian function $\mathcal{L}$. To achieve this target, we first consider the infimum of $\alpha_{ij} \left\| \boldsymbol{Y}_{ij} \right\|_2 + \boldsymbol{\nu}_{ij}^T \boldsymbol{Y}_{ij}$ following the ideas in [35].

Proposition 1. *For any $\boldsymbol{Y}_{ij}$ that minimizes $\mathcal{L}$, we have*

$$\inf_{\boldsymbol{Y}_{ij}} \ \alpha_{ij} \left\| \boldsymbol{Y}_{ij} \right\|_2 + \boldsymbol{\nu}_{ij}^T \boldsymbol{Y}_{ij} = \begin{cases} 0 & \left\| \boldsymbol{\nu}_{ij} \right\|_2 \le \alpha_{ij} \\ -\infty & \text{otherwise} \end{cases}$$

for all $(i,j) \in \mathcal{E}$.

According to **Proposition** 1 (which follows the Cauchy-Schwarz inequality), when $\left\| \boldsymbol{\nu}_{ij} \right\|_2 \le \alpha_{ij}$, the rest part of $\mathcal{L}$ (as denoted by $\tilde{\mathcal{L}}$) becomes an unconstrained LP, whose optimality condition can be expressed as:

$$\nabla \tilde{\mathcal{L}}(\boldsymbol{x})|_{\boldsymbol{x}=\boldsymbol{p},\boldsymbol{q},\boldsymbol{P},\boldsymbol{Q},\boldsymbol{v},\boldsymbol{\ell}} = 0 \tag{85}$$

4) Step 4: By maximizing the infimum of $\mathcal{L}$, we derive the dual **OPF-SOCP** as in the following:

$$\begin{aligned}
J_{\rm d} = & \max_{\boldsymbol{\pi},\boldsymbol{\theta},\boldsymbol{\rho},\boldsymbol{\gamma},\boldsymbol{\phi},\boldsymbol{\sigma},\boldsymbol{\varsigma},\boldsymbol{\omega}} \ \inf_{\boldsymbol{p},\boldsymbol{q},\boldsymbol{P},\boldsymbol{Q},\boldsymbol{v},\boldsymbol{\ell}} \mathcal{L} \\
& = \max \sum_{i\in\mathcal{N}^+} \left(\overline{v}_i \gamma_i^u - \underline{v}_i \gamma_i^l\right) + \sum_{(i,j)\in\mathcal{E}} \overline{\ell}_{ij} \rho_{ij} \\
& + \sum_{i\in\mathcal{N}^+} \left(\overline{p}_i \phi_i^u - \underline{p}_i \phi_i^l + \overline{q}_i \varphi_i^u - \underline{q}_i \varphi_i^l \right)
\end{aligned} \tag{86}$$

$$s.t. \ \pi_i + \phi_i^u - \phi_i^l = 0, \quad \forall i \in \mathcal{N}^+ \tag{87}$$

$$\tau_i + \varphi_i^u - \varphi_i^l = 0, \quad \forall i \in \mathcal{N}^+ \tag{88}$$

$$\pi_0 = 0 \tag{89}$$

$$\tau_0 = 0 \tag{90}$$

$$\pi_j - \pi_i - 2r_{ij}\theta_{ij} + \sigma_{ij} = 0, \quad \forall (i,j) \in \mathcal{E} \tag{91}$$

$$\tau_j - \tau_i - 2x_{ij}\theta_{ij} + \varsigma_{ij} = 0, \quad \forall (i,j) \in \mathcal{E} \tag{92}$$

$$\theta_{ij} - \sum_{k:k\to i} \theta_{ki} + \gamma_i^u - \gamma_i^l - \kappa_{ij} + \omega_{ij} \le 0, \quad \forall i \in \mathcal{N}^+ \tag{93}$$

$$\begin{aligned}
-(r_{ij}\pi_j + x_{ij}\tau_j) + (r_{ij}^2 + x_{ij}^2)\theta_{ij} + \rho_{ij} + \kappa_{ij} + \omega_{ij} \le r_{ij}, \\
\forall (i,j) \in \mathcal{E}
\end{aligned} \tag{94}$$

$$\left\| \begin{matrix} \sigma_{ij} \\ \varsigma_{ij} \\ \kappa_{ij} \end{matrix} \right\|_2 \le \omega_{ij}, \quad \forall (i,j) \in \mathcal{E} \tag{95}$$

Note that $\sum_{(i,j)\in\mathcal{E}} y_{ij} \left(\omega_{ij} - \alpha_{ij}\right)$ is minimized if and only if $\alpha_{ij} = \omega_{ij}$ for all $(i,j) \in \mathcal{E}$. So the optimality condition in **Proposition** 1 is equivalent to $\left\| \boldsymbol{\nu}_{ij} \right\|_2 \le \omega_{ij}$. Together with (84), we have the dual SOCP constraints as in (95).

REFERENCES

[1] R. A. Jabr, "Radial distribution load flow using conic programming," *IEEE Transactions on Power Systems*, vol. 21, no. 3, pp. 1458–1459, 2006.

[2] S. Bose, S. H. Low, T. Teeraratkul, and B. Hassibi, "Equivalent relaxations of optimal power flow," *IEEE Transactions on Automatic Control*, vol. 60, no. 3, pp. 729–742, 2015.

[3] Z. Miao, L. Fan, H. G. Aghamolki, and B. Zeng, "Least squares estimation based SDP cuts for SOCP relaxation of AC OPF," *IEEE Transactions on Automatic Control*, vol. 63, no. 1, pp. 241–248, 2017.

[4] M. Nick, R. Cherkaoui, J.-Y. Le Boudec, and M. Paolone, "An exact convex formulation of the optimal power flow in radial distribution networks including transverse components," *IEEE Transactions on Automatic Control*, vol. 63, no. 3, pp. 682–697, 2017.

[5] X. Bai, H. Wei, K. Fujisawa, and Y. Wang, "Semidefinite programming for optimal power flow problems," *International Journal of Electrical Power and Energy Systems*, vol. 30, no. 6-7, pp. 383–392, 2008.

[6] J. Lavaei and S. H. Low, "Zero duality gap in optimal power flow problem," *IEEE Transactions on Power Systems*, vol. 27, no. 1, pp. 92–107, 2012.

[7] M. Farivar and S. H. Low, "Branch flow model: Relaxations and convexification-Part I," *IEEE Transactions on Power Systems*, vol. 28, no. 3, pp. 2554–2564, 2013.

[8] S. H. Low, "Convex relaxation of optimal power flow-Part II: Exactness," *IEEE Transactions on Control of Network Systems*, vol. 1, no. 2, pp. 177–189, 2014.

[9] L. Gan, N. Li, U. Topcu, and S. H. Low, "Exact convex relaxation of optimal power flow in radial networks," *IEEE Transactions on Automatic Control*, vol. 60, no. 1, pp. 72–87, 2015.

[10] C. Lin, W. Wu, B. Zhang, B. Wang, W. Zheng, and Z. Li, "Decentralized reactive power optimization method for transmission and distribution networks accommodating large-scale DG integration," *IEEE Transactions on Sustainable Energy*, vol. 8, no. 1, pp. 363–373, 2017.

[11] H. Haghighat and B. Zeng, "Stochastic and chance-constrained conic distribution system expansion planning using bilinear Benders decomposition," *IEEE Transactions on Power Systems*, vol. 33, no. 3, pp. 2696–2705, 2018.

[12] Z. Wu, Y. Liu, W. Gu, J. Zhou, J. Li, and P. Liu, "Decomposition method for coordinated planning of distributed generation and distribution network," *IET Generation, Transmission and Distribution*, vol. 12, no. 20, pp. 4482–4491, 2018.

[13] Z. Lin, Z. Hu, H. Zhang, and Y. Song, "Optimal ESS allocation in distribution network using accelerated generalised Benders decomposition," *IET Generation, Transmission and Distribution*, vol. 13, no. 13, pp. 2738–2746, 2019.

[14] H. Sekhavatmanesh and R. Cherkaoui, "A novel decomposition solution approach for the restoration problem in distribution networks," *IEEE Transactions on Power Systems*, vol. 35, no. 5, pp. 3810–3824, 2020.

[15] T. Ding, C. Li, C. Zhao, and M. Wang, "Total supply capability considering distribution network reconfiguration under N-k transformer contingency and the decomposition method," *IET Generation, Transmission and Distribution*, vol. 11, no. 5, pp. 1212–1222, 2016.

[16] V. Kekatos, G. Wang, A. J. Conejo, and G. B. Giannakis, "Stochastic reactive power management in microgrids with renewables," *IEEE Transactions on Power Systems*, vol. 30, no. 6, pp. 3386–3395, 2014.

[17] X. Wu, A. J. Conejo, and N. Amjady, "Robust security constrained ACOPF via conic programming: Identifying the worst contingencies," *IEEE Transactions on Power Systems*, vol. 33, no. 6, pp. 5884–5891, 2018.

[18] H. Haghighat and B. Zeng, "Bilevel conic transmission expansion planning," *IEEE Transactions on Power Systems*, vol. 33, no. 4, pp. 4640–4642, 2018.

[19] C. Lee, C. Liu, S. Mehrotra, and Z. Bie, "Robust distribution network reconfiguration," *IEEE Transactions on Smart Grid*, vol. 6, no. 2, pp. 836–842, 2015.

[20] M. Yan, X. Ai, M. Shahidehpour, Z. Li, J. Wen, S. Bahramira, and A. Paaso, "Enhancing the transmission grid resilience in ice storms by optimal coordination of power system schedule with pre-positioning and routing of mobile DC de-icing devices," *IEEE Transactions on Power Systems*, vol. 34, no. 4, pp. 2663–2674, 2019.

[21] H. Ji, C. Wang, P. Li, F. Ding, and J. Wu, "Robust operation of soft open points in active distribution networks with high penetration of photovoltaic integration," *IEEE Transactions on Sustainable Energy*, vol. 10, no. 1, pp. 280–289, 2019.

[22] H. Gao, J. Liu, and L. Wang, "Robust coordinated optimization of active and reactive power in active distribution systems," *IEEE Transactions on Smart Grid*, vol. 9, no. 5, pp. 4436–4447, 2018.

[23] T. Ding, C. Li, Y. Yang, J. Jiang, Z. Bie, and F. Blaabjerg, "A two-stage robust optimization for centralized-optimal dispatch of photovoltaic inverters in active distribution networks," *IEEE Transactions on Sustainable Energy*, vol. 8, no. 2, pp. 744–754, 2017.

[24] Y. He, M. Shahidehpour, Z. Li, C. Guo, and B. Zhu, "Robust constrained operation of integrated electricity-natural gas system considering distributed natural gas storage," *IEEE Transactions on Sustainable Energy*, vol. 9, no. 3, pp. 1061–1071, 2018.

[25] Y. Li, Z. Li, F. Wen, and M. Shahidehpour, "Minimax-regret robust co-optimization for enhancing the resilience of integrated power distribution and natural gas systems," *IEEE Transactions on Sustainable Energy*, vol. 11, no. 1, pp. 61–71, 2020.

[26] E. D. Andersen, C. Roos, and T. Terlaky, "Notes on duality in second order and p-order cone optimization," *Optimization: A Journal of Mathematical Programming and Operations Research*, vol. 51, no. 4, pp. 627–643, 2002.

[27] L. Tunçel and H. Wolkowicz, "Strong duality and minimal representations for cone optimization," *Computational Optimization and Applications*, vol. 53, no. 2, pp. 619–648, 2012.

[28] Z. Li, J. Wang, H. Sun, F. Qiu, and Q. Guo, "Robust estimation of reactive power for an active distribution system," *IEEE Transactions on Power Systems*, vol. 34, no. 5, pp. 3395–3407, 2019.

[29] X. Cao, J. Wang, and B. Zeng, "Networked microgrids planning through chance constrained stochastic conic programming," *IEEE Transactions on Smart Grid*, vol. 10, no. 6, pp. 6619–6628, 2019.

[30] X. Cao, J. Wang, J. Wang, and B. Zeng, "A risk-averse conic model for networked microgrids planning with reconfiguration and reorganizations," *IEEE Transactions on Smart Grid*, vol. 11, no. 1, pp. 696–709, 2020.

[31] M. Baran and F. F. Wu, "Optimal sizing of capacitors placed on a radial distribution system," *IEEE Transactions on Power Delivery*, vol. 4, no. 1, pp. 735–743, 1989.

[32] M. Baran and F. Wu, "Optimal capacitor placement on radial distribution systems," *IEEE Transactions on Power Delivery*, vol. 4, no. 1, pp. 725–734, 1989.

[33] Z. Tian, W. Wu, B. Zhang, and A. Bose, "Mixed-integer second-order cone programing model for VAR optimisation and network reconfiguration in active distribution networks," *IET Geneneration, Transmission and Distribution*, vol. 10, no. 8, pp. 1938–1946, 2016.

[34] A. Ben-Tal and A. Nemirovski, *Lectures on modern convex optimization: Analysis, algorithms, and engineering applications*. SIAM, 2001, vol. 2.

[35] S. Boyd and L. Vandenberghe, *Convex Optimization*. Cambridge University Press, 2004.

[36] T. Ding, "Cases for radial network," 2014. [Online]. Available: http://shgl.curent.utk.edu/toolsdemo/

[37] X. Cao, T. Cao, F. Gao, and X. Guan, "Risk-averse storage planning for improving RES hosting capacity under uncertain siting choice," *IEEE Transactions on Sustainable Energy*, Early Access, 2021.

Xiaoyu Cao (S'17, M'19) received the Ph.D. degree in electrical engineering from Xi'an Jiaotong University, Xi'an, China, in 2019. He is currently an Assistant Professor with Systems Engineering Institute, the School of Automation Science and Engineering of Xian Jiaotong University, Xi'an, China. His current research interests include microgrids planning and scheduling, energy system resilience, and stochastic mixed-integer program with applications in smart grid and energy internet.

Jianxue Wang (M'11, SM'18) received the B.S., M.S., and Ph.D. degrees in electrical engineering from Xi'an Jiaotong University, Xi'an, China, in 1999, 2002, and 2006, respectively. He is currently a Professor at the School of Electrical Engineering in Xi'an Jiaotong University. His research interests include power system planning and scheduling, microgrid planning and schdeuling, and electricity market.

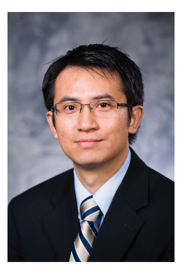

Bo Zeng (M'11) received the Ph.D. degree in industrial engineering from Purdue University, West Lafayette, IN, USA. He currently is an Associate Professor with the Department of Industrial Engineering, and the Department of Electrical and Computer Engineering, University of Pittsburgh, Pittsburgh, PA, USA. His research interests include polyhedral study and algorithms for stochastic and robust mixed integer programs, coupled with applications in power and logistics systems. He is also a member of IISE and INFORMS.